Phase diagram of magnetic multilayers: The role of biquadratic exchange

N. S. Almeida* and D. L. Mills
Department of Physics and Astronomy, University of California, Irvine, California 92717-4575
(Received 16 June 1995)

We study the magnetic phase diagram of a superlattice fabricated from ferromagnetic films, with interfilm exchange coupling provided by intervening nonferromagnetic layers. We suppose the interfilm exchange coupling contains a biquadratic component, with magnitude comparable to the linear exchange, as found recently in the Fe/Cr(211) structures. Our analysis centers on these materials, where the Fe magnetizations lie in plane, which also contains a twofold anisotropy axis. Sufficiently large biquadratic exchange produces important qualitative modifications of the magnetization curves, and can introduce new magnetic phases. We illustrate with results for infinite superlattices, and for finite superlattices with either an even or odd number of ferromagnetic layers.

I. INTRODUCTION

When ferromagnetic films are incorporated into magnetic multilayers or superlattices, there are magnetic interactions between adjacent ferromagnetic films, mediated by the spacer layer between them. These have the character of exchange interactions of Heisenberg form, for most systems studied so far. One may thus write the interaction energy between adjacent films in the form $H_x\hat{\mathbf{n}}_1\cdot\hat{\mathbf{n}}_2$, with $\hat{\mathbf{n}}_1$ and $\hat{\mathbf{n}}_2$ unit vectors parallel to the magnetization of the appropriate films. Here H_x measures the energy difference between parallel and antiparallel alignments of adjacent films. The coupling constant H_x can be either positive (antiferromagnetic coupling) or negative (ferromagnetic coupling). It is by now well known that H_x oscillates in sign as the spacer layer thickness increases.[1] The exchange coupling just described, in combination with the anisotropy and external magnetic fields, can lead to rich magnetic phase diagrams. This is illustrated by recent studies[2–4] of newly synthesized Fe/Cr(211) superlattices.

It has been recognized recently that the interfilm exchange coupling can be more complex than described above. In the near vicinity of spacer thicknesses for which H_x changes sign, 90° orientations of the magnetization of the ferromagnetic constituents of Fe/Cr/Fe trilayers were reported by Rühring *et al.*[5] These authors argued that this requires the presence of biquadratic coupling between adjacent films we write as $H_b(\hat{\mathbf{n}}_1\cdot\hat{\mathbf{n}}_2)^2$ where $H_b>0$. Shortly after this experimental discovery of biquadratic exchange, Slonczewski[6] proposed an extrinsic mechanism which leads to biquadratic exchange, for the system studied in Ref. 5. Model calculations illustrate that there are intrinsic mechanisms as well.[7] A recent review of intrinsic and extrinsic mechanisms that lead to both linear and biquadratic exchange has been provided by Slonczewski.[8]

Until recently, biquadratic exchange has been found to be rather weak, compared to the linear exchange H_x. It is for this reason that biquadratic exchange asserts itself only for those spacer thicknesses close to zeros in H_x. However, it is the case that for the Fe/Cr(211) structures, one may synthesize samples for which H_b is very large, comparable to H_x itself.[9] For such materials, we may expect phase diagrams and magnetization curves very different than those discussed previously.

This paper is devoted to a theoretical study of the influence of biquadratic exchange on the phase diagram of magnetic superlattices. We find its presence indeed leads to striking effects, including new magnetic phases with magnetization in the ground state parallel to the hard direction. We consider first a superlattice of infinite extent in Sec. II then turn to finite superlattices in Sec. III.

II. INFINITE SUPERLATTICE

We consider an infinitely extended superlattice, whose magnetic constituents are thin ferromagnetic films, with magnetization inplane. We take this to be the x-z plane. As the spins reorient in response to an external magnetic field, the magnetization always lies in the x-z plane. The very strong demagnetization field generate by tipping the magnetization out of plane will suppress any tendency for the magnetization to tilt out of plane. Let $\hat{\mathbf{n}}_i$ be a unit vector in the direction of the magnetization of the ith film. We explore the properties of the energy functional

$$E(\{n_i\})=\tfrac{1}{2}H_x\sum_i \hat{\mathbf{n}}_i\cdot\hat{\mathbf{n}}_{i+1}+\tfrac{1}{2}H_b\sum_i (\hat{\mathbf{n}}_i\cdot\hat{\mathbf{n}}_{i+1})^2$$
$$-\tfrac{1}{2}H_a\sum_i (\hat{\mathbf{n}}_i^z)^2-H_0\sum_i \hat{\mathbf{n}}_i^z. \qquad (2.1)$$

Here energies are measured in units of magnetic field. The first term is the conventional linear exchange, which is antiferromagnetic when $H_x>0$. We confine our attention here to the case $H_x>0$. The second term is the biquadratic exchange. Experimentally, one finds $H_b>0$. The third term is the uniaxial anisotropy, which renders the z direction an easy direction. For the moment, we assume an external magnetic field H_0 is applied along the easy axis.

When $H_b=0$ we recover the energy functional used in earlier work.[2,3] In this limit, the magnetic phase diagram of

the superlattice is identical to that of the classical two-sublattice antiferromagnets such as MnF_2 and FeF_2. For low applied fields H_0, we have a simple antiferromagnetic ground state. As H_0 is increased, when H_0 reaches $H_c^{(1)}=[H_a(2H_x-H_a)]^{1/2}$, there is a first-order magnetic-field-induced phase transition to the spin-flop state. As H_0 is increased further, one reaches the saturated ferromagnetic state when $H_0=H_c^{(2)}=2H_x-H_a$. Just at saturation, a second-order phase transition is realized. This picture applies for $H_a<H_x$, a limit for the systems of interest here. For $H_a>H_x$, there is no spin-flop phase, but one passes directly from the antiferromagnetic ground state to the saturated state. In the finite superlattice and for an even number of layers, one realizes the surface spin-flop state when $H_b=0$, as confirmed by experimental studies of Fe/Cr(211) structures.[2]

We shall assume that in the presence of biquadratic exchange we still have a two sublattice configuration at all fields. However, we allow for the possibility of an asymmetric state, which we shall see is realized if H_b is sufficiently large. Thus, for all odd-numbered films, we let $\hat{\mathbf{n}}_i=\hat{x}\cos(\beta_1)+\hat{z}\sin(\beta_1)$ and for all even numbered films we let $\hat{\mathbf{n}}_i=\hat{x}\cos(\beta_2)+\hat{z}\sin(\beta_2)$. The choice $\beta_1=-\beta_2$ generates the classical spin-flop state of the two-sublattice antiferromagnet.

By requiring the energy functional to be an extremum, we find we must solve the set of equations

$$H_x\sin(\beta_1-\beta_2)+H_b\sin[2(\beta_1-\beta_2)]-\tfrac{1}{2}H_a\sin(2\beta_1)-H_0\sin(\beta_1)=0 \tag{2.2a}$$

and

$$H_x\sin(\beta_1-\beta_2)+H_b\sin[2(\beta_1-\beta_2)]+\tfrac{1}{2}H_a\sin(2\beta_2)+H_0\sin(\beta_2)=0. \tag{2.2b}$$

These equations always yield the antiferromagnetic (AFM) state, where $\beta_1=0$ and $\beta_2=\pi$ or conversely, and the ferromagnetically (FM) aligned state $\beta_1=\beta_2=0$. We also have a ferromagnetic state with all moments antiparallel to the field, but of course this state is always unstable.

It is possible to extract some information on the phase of the system and its stability, through analytic methods. A given phase is stable if the matrix $\partial^2E/\partial\beta_1\partial\beta_2$ has positive eigenvalues. We will encounter first-order magnetic-field-induced phase transitions, in our final phase diagram. There is necessarily hysteresis near such a phase transition. A phase may be locally stable by the criterion just stated, while at the same time there is a second phase of lower energy, under this circumstance.

By analytical means, one may show that the low-field antiferromagnetic state ($\beta_1=0$, $\beta_2=\pi$) is stable for external fields $H_0<[2H_a(H_x-2H_b)+H_a^2]^{1/2}$, provided $H_b<(2H_x+H_a)/4=H_c^{(AF)}$. Similarly, the ferromagnetically aligned state is stable when $H_0\geq 2(H_x+2H_b)-H_a=H_c^{(FM)}$ for any choice of H_b.

We also can realize a symmetric spin-flop configuration for fields H_0 below $H_c^{(FM)}$. This state has $\beta_1=-\beta_2=\theta$, and is stable whenever

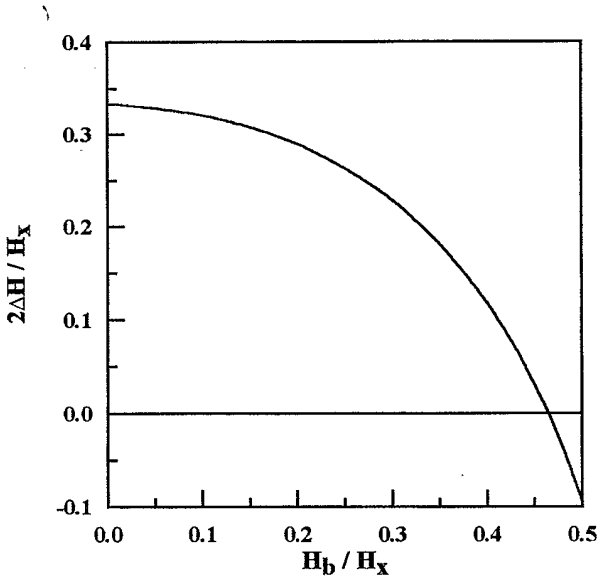

FIG. 1. Variations of the field $\Delta H=H_c^{(AF)}-H_c^{(SF)}$ as a function of the strength H_b of the biquadratic exchange. The low-field antiferromagnetic state is stable for external fields $H_0<H_c^{(SF)}$, and the spin-flop state is stable for $H_0<H_c^{(AF)}$. We have chosen $H_x=2$ kG and $H_a=0.5$ kG for this calculation.

$$\lambda_\pm=A_{11}\pm|A_{12}|\geq 0, \tag{2.3}$$

where

$$A_{11}=(H_a-H_x)\cos(2\theta)-2H_b\cos(4\theta)+H_0\cos(\theta) \tag{2.4}$$

and

$$A_{12}=H_x\cos(2\theta)+2H_b\cos(4\theta). \tag{2.5}$$

Here θ is determined as stated above and is found by solving

$$H_b\cos^3(\theta)+(2H_x-4H_b-H_a)\cos(\theta)-H_0=0. \tag{2.6}$$

From the criteria stated in Eq. (2.3), we can find the smallest external field necessary to stabilize the spin-flop configuration, for any given choice of parameters.

So our results can be set alongside earlier studies of the phase diagram,[2,3] for our quantitative calculations we shall choose $H_x=2$ kG and $H_a=0.5$ kG. If we call the smallest field necessary to stabilize the spin-flop state $H_c^{(SF)}$, we find $H_c^{(SF)}<H_c^{(AF)}$ for $H_b\leq H_b^{(c)}$, where $H_b^{(c)}\cong(H_x-3H_a)/2$. The difference $\Delta H=H_c^{(AF)}-H_c^{(SF)}$ is the width of the region within which both the spin-flop state and the low-field antiferromagnetic state are stable. As we increase H_b, ΔH decreases. This difference approaches zero, to vanish as $H_b\to H_b^{(c)}$ from below, and is negative for $H_b>H_b^{(c)}$. We show the behavior of ΔH as a function of H_b in Fig. 1. We see, for the parameters chosen, $H_b^{(c)}\cong 0.46$ kG.

When we have $H_b>H_b^{(c)}$, it is no longer possible to have a scenario where one has a transition from a low-field antiferromagnetic state to an intermediate state with the character of a spin-flop phase. This is because when $\Delta H<0$, the field regime for which the AF state is stable lies below the lowest field for which the SF phase is stable. As we see, there

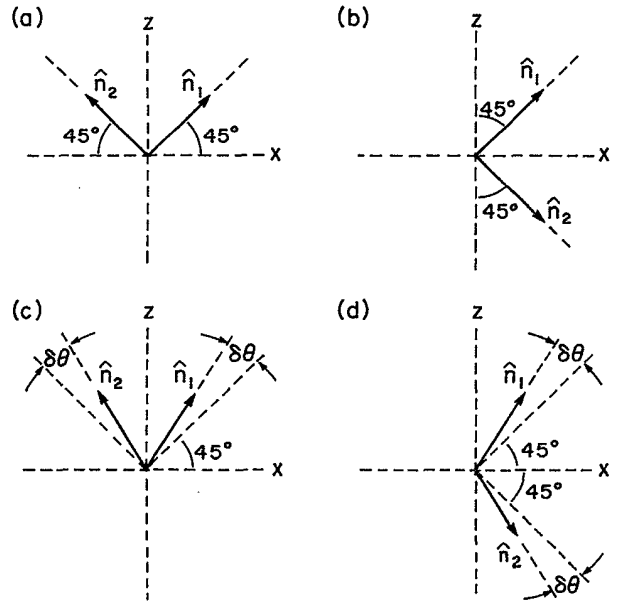

FIG. 2. In (a)–(d), we illustrate magnetic configurations of the infinite superlattice appropriate to the case where the biquadratic exchange H_b is large.

is thus a magnetic field gap of width $|\Delta H|$ within which *neither* the antiferromagnetic *nor* the spin-flop phase is stable. A new phase must enter the phase diagram. Below we outline the nature of this phase, which we find striking, and show how it enters the phase diagram.

The nature of the new phase may be appreciated by supposing the external field H_0 is zero, and also that H_b is very much larger than both H_a and H_x. With H_b only present, clearly the angle between $\hat{\mathbf{n}}_1$ and $\hat{\mathbf{n}}_2$ must be $\pi/2$, as found in the studies which first noted the importance of biquadratic exchange in magnetic multilayers.[5] With H_a and H_x both set to zero at the moment, of course, the energy of the system is unchanged if the pair $\hat{\mathbf{n}}_1$ and $\hat{\mathbf{n}}_2$ are rotated continuously about the axis normal to the film surfaces, as long as the angle between them is maintained at $\pi/2$.

Now we turn on H_a, supposing the linear exchange H_x remains zero. Continue to hold the angle between $\hat{\mathbf{n}}_1$ and $\hat{\mathbf{n}}_2$ at precisely $\pi/2$, for the moment. The presence of the uniaxial anisotropy breaks the rotational symmetry just described. We have two configurations with precisely the same energy, as illustrated in Figs. 2(a) and 2(b). Of course, with $H_a \neq 0$ and the angle between $\hat{\mathbf{n}}_1$ and $\hat{\mathbf{n}}_2$ held fixed at 90°, quite clearly the two configurations illustrated in Figs. 2(a) and 2(b) are not equilibrium configuration of the moments. When the anisotropy is "turned on," the moments will relax as illustrated in Figs. 2(c) and 2(d), to a lower energy by virtue of with the combination of anisotropy and biquadratic exchange coupling. A short calculation shows that the configuration in Fig. 2(c) is precisely degenerate in energy with that in Fig. 2(d). While imposition of the anisotropy breaks the continuous symmetry present in its absence, a twofold degeneracy remains in its presence.

Now suppose we add the linear exchange H_x, which is antiferromagnetic in sign. The effect of this interaction is to *increase* the angle between $\hat{\mathbf{n}}_1$ and $\hat{\mathbf{n}}_2$, since H_x acting alone would generate a simple antiferromagnetic state. Now if the angle $\delta\theta$ in Fig. 2(d) is increased, there will also be a decrease in anisotropy energy, since $\hat{\mathbf{n}}_1$ and $\hat{\mathbf{n}}_2$ will be more closely aligned with the easy axis. Addition of H_x decreases $\delta\theta$ in Fig. 2(c), and this increases the anisotropy energy. Thus the addition of linear exchange H_x lifts the twofold degeneracy discussed in the previous paragraph. If H_x is antiferromagnetic, as we have seen, for large biquadratic exchange, the ground state will be that illustrated in Fig. 2(d).

This is a remarkably unusual state, in our view. We have a system with an easy axis, but the combination of anisotropy, linear, and biquadratic exchange conspires to produce a ground state with net magnetization perpendicular to the easy axis. It would be intriguing to study properties of this state experimentally.

If the linear exchange H_x is ferromagnetic in sign, then the configuration illustrated in Fig. 2(c) has the lower energy. If H_b is substantial, as we shall illustrate below, the energy difference between the two states is quite modest. A consequence is that for H_x ferromagnetic in sign, a rather weak external field applied normal to the easy axis will induce a "flop" to the state in Fig. 2(d). Conversely, if H_x is antiferromagnetic, a weak field along the easy axis will induce a flop from the state in Fig. 2(d), to that in Fig. 2(c). We thus have a magnetic switch.

To describe the new state, we must solve Eqs. (2.2) for general β_1 and β_2, without restrictions on the symmetry of the resulting state. To do this, we proceed as follows. We let $\xi=\cos(\beta_1-\beta_2)$ and $\alpha=(H_a/2)\sin(2\beta_1)+H_0\sin(\beta_1)$. Upon rearranging Eq. (2.2a) and then squaring, we arrive at

$$(1-\xi^2)(H_x+2H_b\xi)^2=\alpha^2. \tag{2.7}$$

We proceed by guessing a value for β_1, which generates a value for α. We solve Eq. (2.6), a quartic, for the four values of ξ, and from these we obtain eight values of β_2. We check to see if each pair (β_1,β_2) is a solution of Eq. (2.2b). By scanning the input angle β_1, we are able to locate all possible (β_1,β_2) pairs which yield a possible state. The stability of each state is confirmed by diagonalizing the matrix $\partial^2 E/\partial\beta_i\partial\beta_j$, to check for negative eigenvalues. By this means we find, for values of H_0 where neither the antiferomagnetic or spin-flop state is stable, an asymmetric state with magnetization canted away from the easy axis. We construct a phase diagram by searching for the lowest-energy solution for each field H_0. In Fig. 3, for the choice $H_a=0.5$ kG and $H_x=2$ kG, we show the complete magnetic phase diagram of the system. When the biquadratic exchange $H_b=0$, application of the external field takes us from the low-field antiferromagnetic (AF) state, to a spin-flop (SF) state through a first-order magnetic-field-induced phase transition, and then to the saturated ferromagnetic state (FM) state. As is usual in antiferromagnets, the transition from the spin-flop state to the saturated state is second order, accompanied by a discontinuity in (dM/dH).

When $H_b/H_x \geq 0.55$, the ground state in zero field is an asymmetric state very similar to that depicted in Fig. 2(d). We have, as discussed above, a net moment perpendicular to the easy axis. As the external field is applied parallel to the easy axis, a moment is induced along the easy axis by means a rotation in the plane of the "scissors structure" shown in

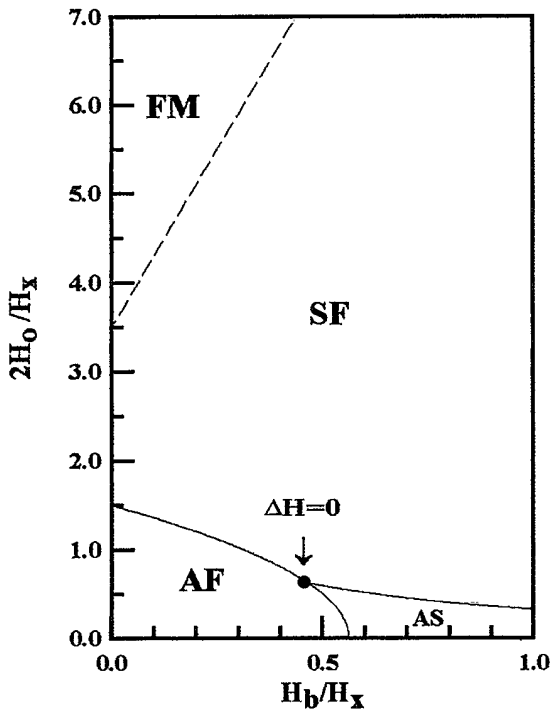

FIG. 3. H_0-H_b magnetic phase diagram of an infinite superlattice with $H_x=2$ kG and $H_a=0.5$ kG. The labels FM, AF, SF, and AS mean ferromagnetic, antiferromagnetic, spin flop, and asymmetric configurations, respectively.

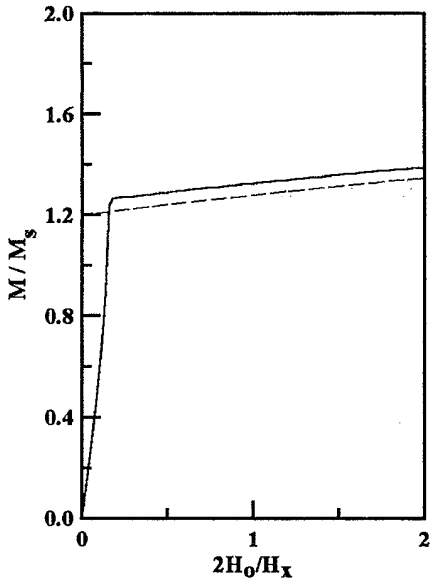

FIG. 4. For the case $H_x=2$ kG, $H_a=0.5$ kG, and $H_b=4$ kG, we show the variation of the magnetization with external field for the case where the field is applied parallel to the easy axis (solid curve), and this is compared to the case where the field is applied perpendicular to the easy axis (dotted curve).

Fig. 2(d). At a certain field, $\hat{\mathbf{n}}_1$ and $\hat{\mathbf{n}}_2$ become symmetrically disposed about the easy axis, in the spin-flop conformation. The transition from the asymmetric configuration to the spin-flop state has the character of a second-order phase transition. Note we have an interesting tricritical point at the value of H_b where the field gap ΔH illustrated in Fig. 1 vanishes. There is a narrow regime of field where we have the antiferromagnetic ground state, and application of an external field triggers a first-order transition to the asymmetric state, followed by a second-order transition to the spin-flop state.

The behavior of the system in the limit where the ratio (H_b/H_x) is large compared to unity is of interest. Arguments given above show that as $H_x \to 0$ (so $H_b/H_x \to \infty$), in zero magnetic field the configurations shown in Figs. 2(c) and 2(d) are degenerate. For finite H_x, and also H_x antiferromagnetic, as we have argued the configuration in Fig. 2(d) has lower energy than that in Fig. 2(c). The energy difference between these two states is rather small, when $(H_b/H_x)>1$. Thus, when we have $H_x<0$ and Fig. 2(d) illustrates the ground state, application of a rather weak external field will rotate the total magnetization to align with the easy axis, as in Fig. 2(c). Once this rotation has occurred, the variation of magnetization with the field is remarkably insensitive to whether the external field is applied parallel or perpendicular to the easy axis. In each case, the field pulls the system to saturation, against the combined effects of the linear and biquadratic exchange.

In Fig. 4, we show the field variation of the magnetization component parallel to the external magnetic field for two cases. For one the magnetic field is parallel to the easy axis, and for the other the magnetic field is perpendicular to the easy axis. The calculations are for $H_b/H_x=2$, and H_x antiferromagnetic in sign. The zero-field ground state is thus that illustrated in Fig. 2(d). When the field is parallel to the easy axis, the magnetization initially increases linearly with field, with $(\partial M/\partial H_0)$ quite large. In this low-field regime, $\hat{\mathbf{n}}_1$ and $\hat{\mathbf{n}}_2$ are rotating, with the angle between them roughly $\pi/2$. At the point where there is a break in slope, $\hat{\mathbf{n}}_1$ and $\hat{\mathbf{n}}_2$ are symmetrically disposed about the easy axis. Above this field, the magnetization is virtually identical for the two external field directions. This is a striking result, in our view. The underlying physics is that of a highly anisotropic magnetic material, yet its macroscopic magnetization is remarkably isotropic, except at the very lowest fields.

If we had chosen the linear exchange to be ferromagnetic in sign, the magnetization curves would be remarkably similar to that in Fig. 4, except the ground state will have the form illustrated in Fig. 2(c). Thus the curve with the break in slope will be that for which the field is applied *normal* to the easy axis. The response will be quite isotropic at higher fields, however, as in the antiferromagnetic case.

This completes our discussion of the influence of biquadratic exchange on the infinitely extended superlattice. Quite clearly, as we have seen, when the biquadratic exchange becomes comparable to the linear exchange, there are major modifications of the response characteristics of these structures.

III. INFLUENCE OF BIQUADRATIC EXCHANGE ON THE FINITE SUPERLATTICE

In Ref. 2, both experimental data and theoretical calculations show that the magnetic phase diagram of finite Fe/Cr(211) is richer than that expected for the idealized in-

finitely long superlattice. Most particularly, if the finite structure contains an even number of layers, in the low-field AF state, if one outermost film has magnetization directed along $+\hat{\mathbf{z}}$, then the second outermost film has magnetization directed along $-\hat{\mathbf{z}}$. If an external magnetic field H_0 is directed along $+\hat{\mathbf{z}}$, the outer film antiparallel to H_0 "flops" at a field well below that required to initiate the spin-flop state throughout the structure. We thus have the surface spin-flop state which evolves into the bulk spin-flop state, by means of the mechanism outlined in Ref. 2. There is thus a dramatic even-odd effect, since a superlattice with an odd number of layers will not display the surface spin-flop phase. Clearly, this scenario will be modified dramatically by the presence of strong biquadratic exchange.

In this section, we explore the influence of biquadratic exchange on the magnetic phase diagram of finite structures with an even and odd number of layers. We have found the numerical calculation reported here to be very demanding for large values of H_b, it should be remarked. Thus we begin by summarizing the scheme we have employed.

We consider the same geometry used to study the infinite superlattices to obtain information on the finite one. Therefore, for a system with N magnetic films, the energy functional is

$$E(\{n_i\})=\tfrac{1}{2}H_x\sum_{i=1}^{N-1}\hat{\mathbf{n}}_i\cdot\hat{\mathbf{n}}_{i+1}+\tfrac{1}{2}H_b\sum_{i=1}^{N-1}<(\hat{\mathbf{n}}_i\cdot\hat{\mathbf{n}}_{i+1})^2 -\tfrac{1}{2}H_a\sum_{i=1}^{N}(\hat{\mathbf{n}}_i^z)^2-H_0\sum_{i=1}^{N-1}\hat{\mathbf{n}}_i^z, \tag{3.1}$$

where the various parameters have the same meaning as in the infinite case. By requiring the energy functional to be an extremum, we find the set of equations

$$\sin(\beta_1-\beta_2)[H_x+2H_b\cos(\beta_1-\beta_2)]-H_a\sin(2\beta_1) -H_0\sin(\beta_1)=0, \tag{3.2a}$$

$$\sin(\beta_{i-1}-\beta_i)[H_x+2H_b\cos(\beta_{i-1}-\beta_i)]-\sin(\beta_i-\beta_{i+1}) \times[H_x+2H_b\cos(\beta_i-\beta_{i+1})] -H_a\sin(2\beta_i)-H_0\sin(\beta_i)=0 \quad \text{for } 2\leq i\leq N-1, \tag{3.2b}$$

and finally

$$\sin(\beta_{N-1}-\beta_N)[H_x+2H_b\cos(\beta_{N-1}-\beta_N)]-H_a\sin(2\beta_N) -H_0\sin(\beta_N)=0. \tag{3.2c}$$

Hence the equilibrium configuration of the system is obtained by searching for solutions from Eq. (3.2). To do this, we let $\xi_1=\cos(\beta_1-\beta_2)$ and $\alpha_1=H_a\sin(2\beta_1)+H_0\sin(\beta_1)$ to rewrite Eq. (3.2a)

$$(1-\xi_1^2)(H_x+2H_b\xi_1)^2=\alpha_1^2. \tag{3.3}$$

We select a trial value of β_1, and then Eq. (3.3) gives four values for ξ_1 from which one obtains eight possible values for β_2. We choose the value of β_2 that gives the smallest value for the energy of the first two pairs of films, by examining

$$E_1=H_x\cos(\beta_1-\beta_2)+H_b\cos^2(\beta_1-\beta_2)-H_b[\cos^2(\beta_1) +\cos^2(\beta_2)]-2H_0[\cos^2(\beta_1)+\cos^2(\beta_2)]. \tag{3.4}$$

We continue on by defining, for $2\leq i\leq N-1$, $\xi_i=\cos(\beta_i-\beta_{i+1})$ and $\alpha_i=H_a\sin(2\beta_i)+2H_0\sin(\beta_i) +\sin(\beta_{i-1}-\beta_i)[H_x+2H_b\cos(\beta_{i-1}-\beta_i)]$. Then we rearrange Eq. (3.2b) to read

$$(1-\xi_i^2)(H_x+2H_b\xi_i)^2=\alpha_i^2. \tag{3.5}$$

At this point we know β_i and β_{i-1} and then we calculate the four values of ξ_i that satisfy the Eq. (3.5). From these values of ξ_i we obtain eight values for β_{i+1} and we choose that one that gives the smallest value for

$$E_i=H_x[\cos(\beta_{i-1}-\beta_i)+\cos(\beta_i-\beta_{i+1})]+H_b[\cos^2(\beta_{i-1} -\beta_i)+\cos^2(\beta_i-\beta_{i+1})]-H_a[\cos^2(\beta_i)+\cos^2(\beta_{i+1})] -H_0[\cos(\beta_i)+\cos(\beta_{i+1})]. \tag{3.6}$$

By following the procedure described above, we arrive at the equation for $i=N-1$, where we find β_N which depends on the trial value of β_1. When we find a β_1 value that satisfies the Eq. (3.2c) we have a magnetic configuration $\{\beta_i\}$ that provides an extremum for the energy functional. The equilibrium configuration is one that gives the minimum value for E. The procedure just described provides the set of $\{\beta_i\}$ which minimize the energy.

We used the method described above to obtain the magnetic configuration of finite superlattices with $N=7$ and 8 for different values of H_0. For both superlattices we use $H_x=2$ kG, $H_a=0.5$ kG as in Sec. II. We remark that it has proved difficult for us to generate accurately determined configurations for larger finite structures, when H_b is large. However, these values of N are sufficiently large for us to appreciate the nature of the modifications provided by the biquadratic exchange.

In Fig. 5 for the case $N=8$, we show the variation of the magnetization of the finite superlattice, as a function of external field H_0, for several values of the ratio $R_H=H_b/H_x$. The solid lines give the component of magnetization parallel to the easy axis. For $R_H=0.8$, we have a state where the net magnetization is canted away from the easy axis in low field. The dotted line gives the magnitude of the total magnetization. For $R_H=H_b=0$, the results are quite similar to those presented in Ref. 2, for the superlattice with $N=16$ layers.[10] The magnetization is zero in the low-field antiferromagnetic state, until the surface spin-flop transition is initiated near $H_0\cong 0.9$ kOe. The fine structure present above the onset of the surface spin-flop state has its origin in the domain wall jumps discussed in Ref. 2. The system evolves into a bulk spin-flop configuration out of the surface spin-flop state, again as discussed earlier.

The inclusion of biquadratic exchange initially lowers the threshold for nucleation of the surface spin-flop phase, as we see from the curves in Fig. 5 labeled $R_H=0.2$ and $R_H=0.4$. By the time we reach $R_H=0.8$, the ground state is no longer the antiferromagnetic state. We have a configuration similar to that discussed in Sec. II, where in zero field the net magnetization is along the hard direction. Application of an external field initially twists the film magnetizations,

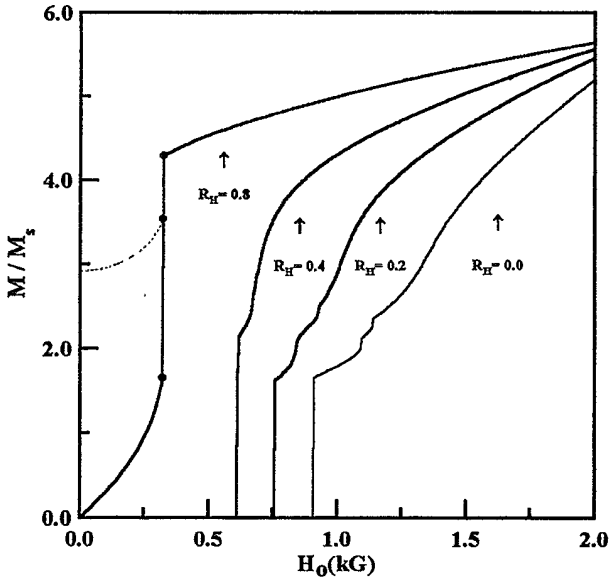

FIG. 5. Variation of the magnetization of a finite superlattice with eight films as a function of external field H_0 for $H_x=2$ kG, $H_a=0.5$ kG, and different values of $R_H=H_b/H_x$. The dotted curve is the variation of the magnitude of the total magnetization for $R_H=0.8$.

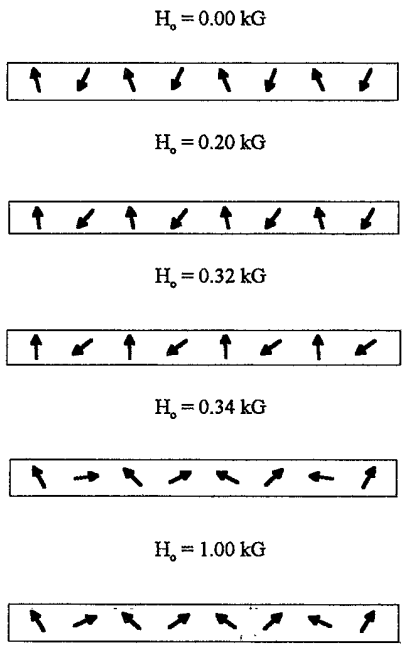

FIG. 6. Equilibrium configurations of the magnetization of the constituent films of the finite superlattice of the Fig. 5, for $R_H=0.8$ and different values of H_0.

and so the structure acquires a net moment parallel to the easy axis. Thus, at least initially, we have a linear susceptibility for the structure in the asymmetric ground state.

As we increase H_0 further, we reach a critical field where there is a discontinuous jump in magnetization. This is produced by a discontinuous jump in the orientation of the magnetizations of the one outmost film, which has the consequence that the system makes a first-order transition from an asymmetric to a symmetric state. We summarize the evolution of the magnetization of the constituent films in Fig. 6. Compare the spin arrangement with $H_0=0.34$ kOe with that for $H_0=0.32$ kOe, to see the transition to the symmetric state.

For an odd number of layers, $N=7$, we show in Fig. 7 the evolution of the component of magnetization along the easy axis (solid lines) and the total magnetization (dotted line) as a function of H_0, for the values of $R_H=H_b/H_x$ used for the even case. For $R_H=0$, the system remains in the antiferromagnetic ground state until the bulk spin-flop transition is initiated at $H_0=1.5$ kOe. The addition of biquadratic exchange initially lowers the threshold field for initiation of the bulk spin flop. At $R_H=0.4$, we find no first-order jump in the magnetization. In effect, the first-order jump decreases in magnitude with increasing R_H, until we reach the point where it vanishes. We then find, as far as we can tell from numerical work, $(\partial M_z/\partial H_0)$ very large, and possibly infinite at threshold. We again have a canted state at $R_H=0.8$, with the magnetization nearly, but not quite, parallel to the hard axis. We illustrate the film magnetization orientation for various fields in Fig. 8. At zero field, we have a canted spin-flop-like state, but with the two sublattices canted about the hard, rather than easy axis. Application of H_0 pulls those spins with $M_z>0$ into alignment with the field, as we see from the panel labeled $H_0=0.26$ kOe. Once these moments achieve alignment, further increases in H_0 bring the downward pointing moment into alignment, and the resulting torques lead to canting of the upward pointing moments; so the system evolves into a state similar to a spin-flop state, where now the two sublattices are arranged (almost) symmetrically about the easy axis, as illustrated in panel labeled $H_0=1.0$ kOe.

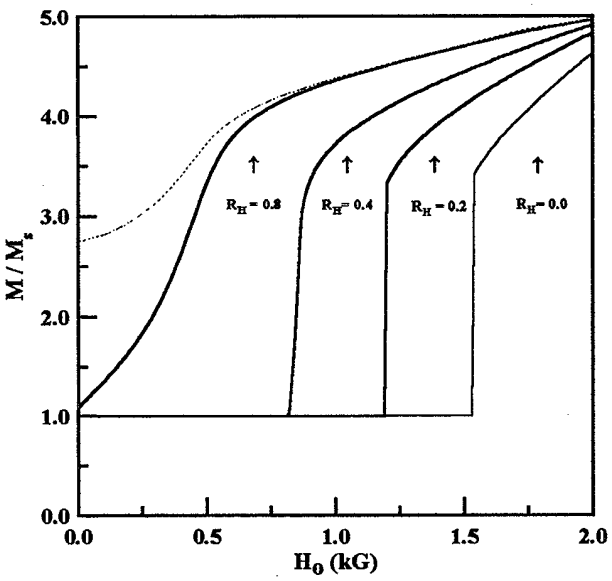

FIG. 7. Variation of the magnetization of a finite superlattice with seven films as a function of external field H_0 for same parameters used in Fig. 5. The dotted curve is the variation of the magnitude of the total magnetization for $R_H=0.8$.

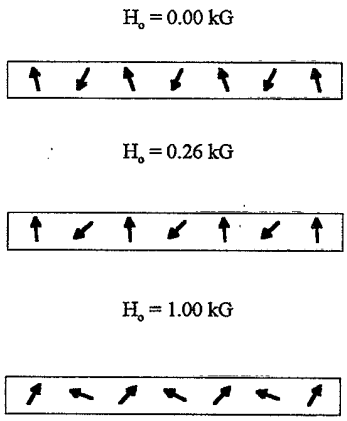

FIG. 8. Equilibrium configurations of the magnetization of the constituent films of the finite superlattice of the Fig. 7, for $R_H=0.8$ and different values of H_0.

The striking "even-odd" effect described in Ref. 2 thus remains in the presence of biquadratic exchange, though if the biquadratic exchange is sufficiently large, we realize intriguing new magnetic configurations.

IV. FINAL REMARKS

Magnetic superlattices such as those modeled and discussed here display a rich and diverse variety of magnetic phases in presence of an external magnetic field. There are dramatic "even-odd" effects for finite structures, which we see persist in the presence of strong biquadratic exchange. The strength of the linear exchange can be controlled or altered through the choice of substrates upon which the films are grown, growth conditions such as temperature, along with the thickness of the ferromagnetic films, and the spacer layers through which the linear and biquadratic exchanges are transmitted.

The calculations reported here, carried out for parameters characteristic of Fe/Cr(211) superlattices, show that the magnetic-field-induced reorientation transitions occur for very modest applied magnetic fields. These structures also exhibit a collective spin-wave spectrum influenced strongly by the relative arrangements of the moments in the various layers. For $H_b=0$, a detailed discussion of these modes has been given elsewhere, for models of the Fe/Cr(211) structure.[3] We thus have a new class of materials, both magnetization curves and response characteristics subject to design. We hope the present results stimulate the detailed study of structures in which the biquadratic and linear exchange are comparable in strength.

ACKNOWLEDGMENTS

This research has been supported by the U.S. Army Research Office, through Contract No. CS001028. N.S.A. also acknowledges the support of the Brazilian Agency CNPq. We appreciate numerous conversations with Dr. E. E. Fullerton and Dr. M. Grimsditch, regarding topics addressed in this paper.

*Permanent address: Departamento de Física Teórica e Experimental, Universidade Federal do Rio Grande do Norte, 59072-970 Natal-RN, Brazil.

[1] S. S. P. Parkin, N. More, and K. P. Roche, Phys. Rev. Lett. **64**, 304 (1990).
[2] R. W. Wang, D. L. Mills, Eric E. Fullerton, J. E. Mattson, and S. D. Bader, Phys. Rev. **72**, 920 (1994).
[3] R. W. Wang and D. L. Mills, Phys. Rev. B **50**, 3931 (1994).
[4] Eric E. Fullerton, M. J. Conover, J. E. Mattson, C. H. Sowers, and S. D. Bader, Phys. Rev. **48**, 15755 (1993).
[5] M. Rührig, R. Schäfer, A. Hubert, J. A. Wolf, S. Demokritov, and P. Grünberg, Phys. Status Solidi A **125**, 635 (1991).
[6] J. C. Slonczewski, Phys. Rev. Lett. **67**, 3172 (1991).
[7] R. P. Erickson, K. B. Hathaway, and J. R. Cullen, Phys. Rev. B **47**, 2626 (1993).
[8] J. C. Slonczewski (unpublished).
[9] Eric E. Fullerton and M. Grimsditch (private communication).
[10] It should be remarked that in the course of the present study, we have reproduced the results of Ref. 2. However, in Fig. 1(b), the spin arrangement illustrated for the field $H_0=1.094$ kOe is actually appropriate to $H_0=1.194$ kOe. There is a labeling error in the figure.